Ultimate tensile strength of loblolly pine strands using stochastic finite element method

Gi Young Jeong · Daniel P. Hindman

Abstract The purpose of the study was to predict the failure strength of different orientation of wood strands from different growth ring positions under tension loading. Stochastic models were constructed to account for the uncertainty of material properties. The Tsai–Hill criteria were used to predict the ultimate tensile strength (UTS). The UTS results from experimental testing were used to validate the results from models. The difference of UTS between experimental and SFEM ranged from 0.09 to 11.09%. Different stress distributions were found for different orientation strand models, whereas uniform stress distribution was found for homogeneous models. The magnitude of the stress distribution was greater for strands from the growth ring number 11–20. Sensitivity analysis showed that grain orientation and growth ring number influenced the UTS of strands. UTS of strands from growth ring number 1–10 showed strength indexes (X_t, Y_t, and S) as dominant factor, whereas UTS of strands from growth ring number 11–20 showed both strength indexes and stress components (σ_1, σ_2, and τ_{12}) as dominant factors.

G. Y. Jeong
Sustainable Engineered Material Institute, Virginia Polytechnic Institute and State University, 230 Cheatham Hall, Blacksburg, VA 24061-0503, USA
e-mail: gjeong1@vt.edu

D. P. Hindman (✉)
Department of Wood Science and Forest Products, Virginia Polytechnic Institute and State University, Brooks Forest Products Center, 1650 Ramble Road, Blacksburg, VA 24061-0503, USA
e-mail: dhindman@vt.edu

Introduction

The use of wood strand-based composites in structural applications has been increasing. Most wood strands have been prepared from plantation-grown trees. Plantation-grown trees have a short-term rotation time, which results in high production of juvenile wood. Juvenile wood located near the pith has a higher microfibril angle and a thinner cell wall, whereas mature wood located near the bark has a lower microfibril angle and a thicker cell wall [1]. Values for tensile strength, bending modulus of rupture (MOR), and bending modulus of elasticity (MOE) of juvenile wood were less than mature wood due to higher fibril angle, shorter tracheid length, and lower specific gravity [2–5]. Prior to analyzing the effect of juvenile wood strands on the mechanical properties of wood strand-based composites, the rigorous analysis of mechanical properties of wood strands from plantations is required for maximizing wood resources.

Strength of wood materials shows large variation due to the complexity of structure, interaction of failure modes, inherent inhomogeneity, anisotropy, and orientation of grain [6, 7]. A deterministic approach, however, cannot predict the scatter range of the variables, and the use of deterministic analysis can lead to serious misinterpretation, including overestimation of strength, underestimation of strength, and inconclusive reliability level. A probability-based failure prediction of wood is more appropriate to overcome the limitation of deterministic approach. Random properties of wood strands will affect not only stiffness changes of wood strands but also the evaluation of stresses in principal material directions, which are important for failure estimation of wood strands.

A great deal of failure criteria used in composite materials are empirical. Therefore, the failure criteria for wood strands should be developed based on physical failure behavior of

wood strands to avoid underestimating strength. Failure stresses for either earlywood or latewood layers present in wood strands are not acceptable because wood strands usually fail by a combination of earlywood and latewood layer failure. Lumped or averaged strength of earlywood and latewood may provide a more realistic assessment of the failure envelope. To have a more reliable prediction of wood strand strength, the variation of material properties of wood strands should be accounted for as well as statistical variation of failure strength. Kasal and Leichti [8] proposed "The problem of finding the failure probability can be reduced to finding parameters of a multivariate distribution."

Deterministic finite element method (FEM) and stochastic finite element method (SFEM) were employed to analyze the effect of the variation of earlywood and latewood properties and grain orientations on mechanical behavior of wood strands. Homogeneous models were also employed as control for layer models. SFEM counted the variations of earlywood and latewood material properties, and the variation of the wood strengths as random variables for stochastic processing.

Literature review

The computation of the stochastic field of nodal displacements (u) from the random stiffness matrix (K) is the main objective of the SFEM. There are many representative methods to solve the SFEM, including perturbation, Monte Carlo simulation, Neumann expansion, and Karhunen–Loeve decomposition [9–17]. This study focuses on Monte Carlo simulation method to generate the random stiffness matrix (K). The stochastic field of nodal displacements (u) can be expressed in response to the stiffness matrix. Although there was no previous research on strength prediction of wood strands using SFEM, studies for prediction of strength of strand-based composite were available. Therefore, literature review was focused on the prediction of strength of strand-based composite.

Wang and Lam [17] constructed a Monte Carlo simulation-based SFEM to predict UTS of parallel strand-based wood composite. Strength modification factors for different layer models were obtained using Weibull-weakest-link theory and size effect to fit the strength from experimental results. The results associated with strength modification factors from models were agreed with the results from experimental test.

Clouston and Lam [11] used the SFEM to predict the strength of angle ply laminates ([±15]$_s$ and [±30]$_s$). The SFEM predicted the failure indexes for the different angle laminates using Tsai–Wu failure criteria associated with flow rule. The failure index was modified by size effect and loading configuration effect between tension and bending.

The difference of strength between simulation and experimental test results ranged from 3.8 to 9.8%. Clouston [18] expanded the model to count statistical variation of void area and grain angle in parallel strand lumber (PSL) made from Douglas fir (*Pseudotsuga menziesii*). The difference between model and experimental results for tension, compression, and bending strength of the PSL was 5.5, 3.3, and 6.4%, respectively.

Kasal and Leichti [8] summarized the previous studies on application of various failure criteria on wood material. Most deterministic stress analysis assumed wood materials as a homogeneous and isotropic material that violated the real physical structure of wood material. Such simplifications were only acceptable for obtaining primitive results assuming uniaxial stresses involved. Some stochastic analysis application on strength of wood material including first-order second moment method, Monte Carlo simulation method, and Binomial distribution method were summarized.

Jeong [7] measured the strength of different orientation of wood strands from the two different growth ring positions and found the specific distribution of strength values, including longitudinal strength, transverse strength, and shear strength. The distribution of strength of wood strands was used to generate the random strength indexes to predict the ultimate tensile strength (UTS) of different orientation wood strands. The average of the strength values from experimental test were used to validate the predicted UTS from the current models.

The goal of this study was to predict the UTS of different grain orientation strands from growth ring number 1–10 and growth ring number 11–20 using SFEM considering the variability of material properties. Uncertainties of strength indexes were implemented using Monte Carlo simulation with known probabilities of UTS of different grain orientation strands from experimental test result. The sensitivity analysis was conducted to analyze the effect of input random variables on the UTS of different orientation wood strands.

Model development

Figure 1 shows the four different orientation wood strand models, dimensions of the model analogs, and the loading conditions. Models A, B, C, and D were used to represent the different orientation strands from growth ring number 1–10 and growth ring number 11–20. While models A, B, and C were considered variation of intraring properties and grain angles, model D did not include intraring property variation and grain angle effect. The dimension for all deterministic FEM and SFEM models was 10.0 cm in length, 2.54 cm in width, and 0.6 mm in thickness. The ratio of latewood and earlywood was defined to be 0.5.

Fig. 1 Structural analog of strand orientation models
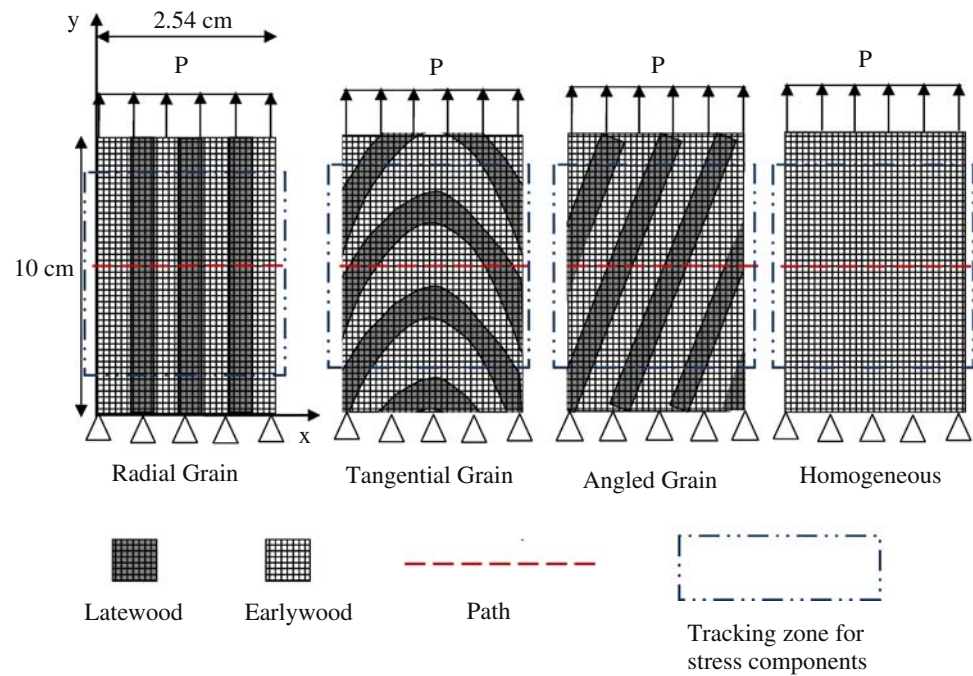
Uniform tension displacement applied at the top end of the strands and at the bottom of the strands was fixed in both x and y direction. A two-dimensional finite element model was used with a plane stress option to apply the thickness for stress calculations.

The following assumptions were made to predict UTS of different orientation strands.

1. Strength indexes are random and independent.
2. Stress components increase linearly with the increment of displacement.
3. Strength and stress components are not correlated.

Deterministic FEM and probabilistic SFEM stress components and strength indexes generation

Table 1 shows the best fitted distribution for strength indexes (X_t, Y_t, and S) from two growth ring numbers with

distribution parameters [7]. The average strength values and standard deviation from experimental and the distribution were also shown. X_t represented transverse strength, Y_t represented longitudinal strength, and S represented shear strength.

For deterministic layer FEM, stress components were obtained using the average material properties for earlywood and latewood from growth ring number 1–10 and growth ring number 11–20. Average strength component for the deterministic models were used to predict the UTS of different orientation strands. For homogeneous model, average stress components were calculated using representative material properties for E_L and v_{LR} for growth ring number 1–10 and growth ring number 11–20 that were calculated combining average E_L of earlywood and latewood based on experimental test using rule of mixture and combining average v_{LR} of earlywood and latewood from experimental test using rule of mixture.

Table 1 Distribution of strength indexes from Jeong [7]

	Estimated average (MPa)	Estimated standard deviation (MPa)	Predicted average (MPa)	Predicted standard deviation (MPa)	Fitted distribution	Theta	Scale	Shape
Growth ring number 1–10								
Y_t	20.52	7.56	20.50	7.48	Weibull	6.55	15.72	1.94
X_t	2.94	1.24	2.95	1.20	Weibull	0	3.32	2.64
S	4.66	1.26	4.73	1.24	Gamma	1.04	0.42	8.80
Growth ring number 11–20								
Y_t	29.03	6.85	29.06	6.45	Weibull	0	31.59	5.17
X_t	2.53	0.83	2.52	0.85	Weibull	0	2.81	3.25
S	4.09	1.07	4.09	1.01	Gamma	0	0.25	16.26

For probabilistic SFEM, Monte Carlo simulation associated with Latin Hypercube Sampling technique was used for generating random strength indexes of different orientation strands characterized by the distribution type and by the distribution parameters (Table 1). One thousand analysis loops were executed to generate random strength indexes for different orientation strands and to obtain random stress components based on the distribution of earlywood and latewood properties from the two different growth ring numbers [6].

The distributions of stress components (σ_1, σ_2, and τ_{12}) were obtained from the SFEM. The local stress components were tracked from the elements in the tracking zone that were away from the loading and fixed boundary (Fig. 1). For radial orientation strands, the stress components were obtained from elements of earlywood and latewood bands separately. The averaged stress values of earlywood and latewood bands were used for predicting UTS. For tangential and angled grain orientation strands, the stress components were obtained from elements of earlywood and latewood bands separately, and the highest stress components were used. The two different ways of tracking stress components for the three different orientation strands were mainly due to the physical failure of strands which was observed from experimental testing.

UTS of radial grain orientation strands did not occur by failure of individual earlywood or latewood band. Often, UTS of radial grain orientation strands occurred when the all earlywood and latewood bands failed through the width. However, UTS of angled and tangential grain orientation strands occurred when individual earlywood or latewood band failed. The physical failure for the different orientation strands were considered when the UTS of different orientation strands were predicted.

The probabilistic failure stress was predicted using Eq. 1 showing the Tsai–Hill failure criteria. Based on analytical distribution of three parameters (X_t, Y_t, and S), random strength indexes were generated using Monte Carlo simulation method.

$$\frac{\sigma_1^2}{X_t^2} + \frac{\sigma_2^2}{Y_t^2} + \frac{\tau_{12}^2}{S^2} - \frac{\sigma_1 \sigma_2}{Y_t^2} \leq 1.0 \tag{1}$$

where σ_1 is the principal stress in radial direction, σ_2 is the principal stress in longitudinal direction, τ_{12} is the principal shear stress, X_t is the transverse strength, Y_t is the longitudinal strength, and S is the shear strength.

Regardless of grain orientation and growth ring positions, most strands failed in a brittle manner. From the stress–displacement, extrapolation of slope would meet the peak load, which can be assumed from the experimental results [7]. The maximum stress can be considered as a function of deflection due to the lack of nonlinear deformation. With the slope, stress components were generated

for model results. From the slope of stress and displacement relationship, the three stresses components could be summarized as a function of displacement and values of slope for the three stress components.

$$\sigma_1 = aX \tag{2a}$$

$$\sigma_2 = bX \tag{2b}$$

$$\tau_{12} = cX \tag{2c}$$

where X is the given displacement (Δ), a is the slope between σ_1 and X, b is the slope between σ_2 and X, and c is the slope between τ_{12} and X.

Substituting Eqs. 2a–c into Eq. 1, Eq. 3 can be written as

$$X^2 \left(\frac{a^2}{X_t^2} + \frac{b^2}{Y_t^2} + \frac{c^2}{S^2} - \frac{ab}{Y_t^2} \right) - 1 \leq 0 \tag{3}$$

From Eq. 3, the strength of different grain orientation strands can be predicted as a function of stochastic constants a, b, and c and stochastic constants of strength indexes. To solve Eq. 3, Newton–Raphson iteration method was used with an established tolerance of 1×10^{-7}.

After all simulations were executed from deterministic FEM, stress distributions for different grain strand models were examined from the path through the width at the center of the specimen. Along the path 60 points were marked to collect the stress values. From probabilistic SFEM, all results were exported to Excel to fit the cumulative probability of UTS and conduct sensitivity analysis using Spearman rank correlation coefficient (r) defined in Eq. 4 between input variables and UTS for different grain orientation strands from different growth ring positions.

$$r = 1 - \frac{6 \sum_{i=1}^{n} d_i^2}{n^3 - n} \tag{4}$$

where d_i is the distance in ranks between an input variable and UTS and n is the number of simulations (1000).

Results and discussion

Table 2 shows the percent difference of model and experimental results from Jeong [7]. Homogeneous models for radial grain orientation strands from growth ring number 1–10 (Radial 1–10), growth ring number 11–20 (Radial 11–20), and for tangential grain orientation strands from growth ring number 1–10 (Tangential 1–10) agreed well with the experimental results (0.15, 0.20, and 0.41% difference, respectively). However, the UTS predictions of other oriented strands were not accurate with the homogeneous model ranging from −23.24 to −157.06%. The homogeneous model predicted the strength of radial grain

Table 2 Comparison of average strengths of wood strands from current SFEM and previous experimental tests from Jeong [7]

Notation	Ex (MPa)	H (MPa)	FEM (MPa)	SFEM (MPa)	Ex vs. H (%)[a]	Ex vs. FEM (%)	Ex vs. SFEM (%)
Radial 1–10	20.52	20.51	20.50	20.50	0.15	0.09	0.09
Radial 11–20	29.03	29.07	29.06	29.06	0.20	−0.14	−0.14
Tangential 1–10	20.58	20.51	19.43	19.43	0.41	5.55	5.55
Tangential 11–20	23.51	29.07	26.11	26.11	−23.24	−11.09	−11.09
Angled 1–10	10.47	20.51	10.50	10.50	−95.70	−0.34	−0.34
Angled 11–20	11.27	29.07	11.08	11.08	−157.06	1.60	1.60

Ex Experimental result, *H* Homogeneous model

[a] Difference (%) = (Experimental result − Model results)/Experimental results × 100%

orientation strands well due to the fact that the strength of strands was determined as a system failure rather than either individual earlywood band or latewood band in different orientation wood strands. Since input for the homogeneous model was applied using Rule of Mixture based on earlywood and latewood properties, the homogeneous model for Radial 1–10 and Radial 11–20 should be the same average stress value obtained from the corresponding layer FEM model.

The deterministic layer FEM models and SFEM models had the same average UTS values for the different orientation strands. In general, both deterministic layer FEM and SFEM models predicted well for the different grain orientation wood strands that ranged from 0.09 to 11.09%. Radial grain orientation strands were influenced little by the orientation of earlywood and latewood due to the prediction of system failure, where a failure of the strand would involve multiple layers of both earlywood and latewood. The highest difference of 11.09% between UTS and predicted UTS from FEM and SFEM for tangential grain orientation models was found. Tangential grain orientation strand models were difficult to model because the geometry of earlywood and latewood bands were created by cutting the tangent to the earlywood and latewood boundary when the wood disk assumed a tapered cylinder (Fig. 1). However, the wood strands show variation in the actual earlywood and latewood bands present in the strands, which may influence the volume fraction of earlywood and latewood as well as the specific geometry associated with the mesh for the tangential grain orientation model in Fig. 1.

The highest difference of 95.7 and 157.06% between UTS and predicted UTS from the homogeneous models for angled grain orientation models of growth ring numbers 1–10 and 11–20 was found, respectively. The geometry of the homogeneous models could not mimic the complicated stress distributions induced by the combination of loading direction with orientation of earlywood and latewood for angled grain orientation strands. However, the mimicked geometry of layered FEM and SFEM for angled grain orientation strands could show the stress distribution in

earlywood and latewood bands that were important to predict the UTS. The difference of UTS between experimental and model results was 0.34% for Angled 1–10 and 1.60% for Angled 11–20.

Stress distributions from different strands

Figure 2 shows the normalized longitudinal stress, *y*, distribution through the width of the center of the strand models (Fig. 1) for different growth ring positions. Earlywood and latewood bands change position with the different orientation through the path. Earlywood bands are two times wider than the latewood bands. For radial, tangential, and angled grain strand models, a smaller band plateau stress distribution indicates the latewood band and a larger band plateau indicates the earlywood band.

The stress distribution of the homogenous model was uniform throughout the width of the strand regardless of growth ring positions. Radial grain orientation models showed the distinctive stress, *y*, distribution showing lower stress in earlywood and higher stress in latewood due to the lower longitudinal elastic modulus of earlywood and the greater longitudinal elastic modulus of latewood. Tangential grain orientation models showed higher stress in latewood at both edges and lower stress in earlywood. Although tangential grain orientation model had a different stress distribution between earlywood and latewood, the magnitude of difference between two bands were the lowest compared to the radial and angled grain orientation models. The angled grain orientation models showed lower stress in earlywood bands than the latewood bands. The magnitude of the stress difference between earlywood and latewood for angled grain model was lower than that of radial grain model. Compared to the stress *x* distribution, the magnitude of stress *y* distribution was about 20 times greater for the strands from growth ring number 1–10 and about 15 times greater for the strands from the growth ring number 11–20. The general trend for stress distribution from different growth ring positions were similar but greater magnitude stress in strands from a higher growth ring positions.

Fig. 2 Stress y distribution from simulation models considering grain orientations and growth ring positions. **a** Growth ring number 1–10. **b** Growth ring number 11–20
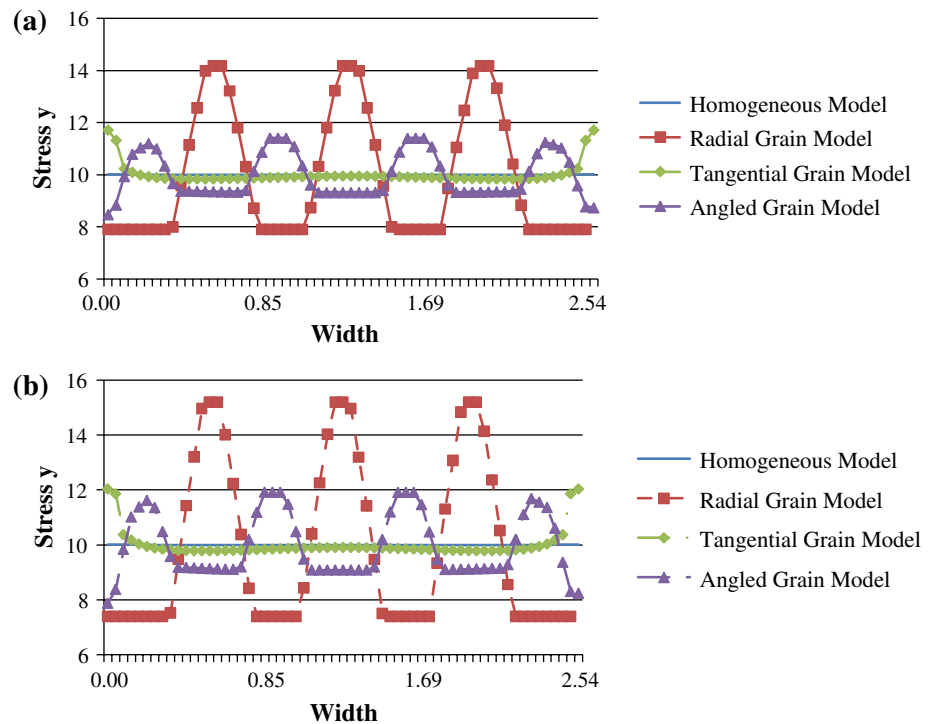
Statistical distribution of the UTS of different orientation of wood strands from different growth ring positions

Figure 3 shows the comparison between cumulative probability of UTS of radial grain orientation models from experimental [7] and predicted UTS from SFEM. A minimum of 30 test results were fitted for experimental cumulative probability of UTS, whereas 1000 simulation results were fitted for SFEM cumulative probability of predicted UTS. Kolmogorov–Smirnov (K–S) test with 95% confidence interval showed that all comparisons between experimental and SFEM were not significantly different.

The two highest differences of 5.55 and 11.09% were found from the comparison for tangential grain orientation strands from growth ring number 1–10 and growth ring number 11–20, respectively (Fig. 3b), also shown in Table 2. The differences for the other models ranged from 0.09 to −1.39%. The two extreme differences were found from the maximum UTS of angled grain orientation strands from growth ring number 1–10 and the minimum predicted UTS of angled grain orientation strand from growth ring number 11–20 (Fig. 3c). While experimental results had maximum UTS of 15.2 MPa from the angled grain orientation strands from growth ring number 1–10, simulation results had maximum predicted UTS of 21.5 MPa. The minimum UTS of angled strands from growth ring 11–20 was 8.2 MPa, whereas the simulation results had a minimum predicted UTS of 2.2 MPa. SFEM models showed more conservative predicted UTS values that covered lowest and highest UTS values from experimental tests.

Radial and tangential grain orientation models showed differences between the 1–10 and 11–20 growth ring numbers for the cumulative probability of predicted UTS, whereas the angled grain orientation models showed no significant difference. The differences of UTS from radial grain orientation models between the 1–10 and 11–20 growth ring numbers and tangential grain orientation models between the 1–10 and 11–20 growth ring numbers could be interpreted as the fact that differences of early-wood and latewood properties between the two growth ring numbers mainly affected the cumulative probability of UTS. UTS values from the angled grain orientation model were not much affected by the difference of earlywood and latewood properties between the two growth ring numbers, but grain orientation did affect the cumulative probability of UTS, which explained grain orientation dominantly affecting the UTS of angled grain orientation, whereas the predicted UTS from radial and tangential grain orientation were mainly affected by earlywood and latewood properties.

Sensitivity analysis for UTS of different grain orientation strands

Table 3 shows Spearman rank correlation coefficient (r) indicating the strength of linear relationship between the random input variables and UTS (Eq. 4). Italicized values
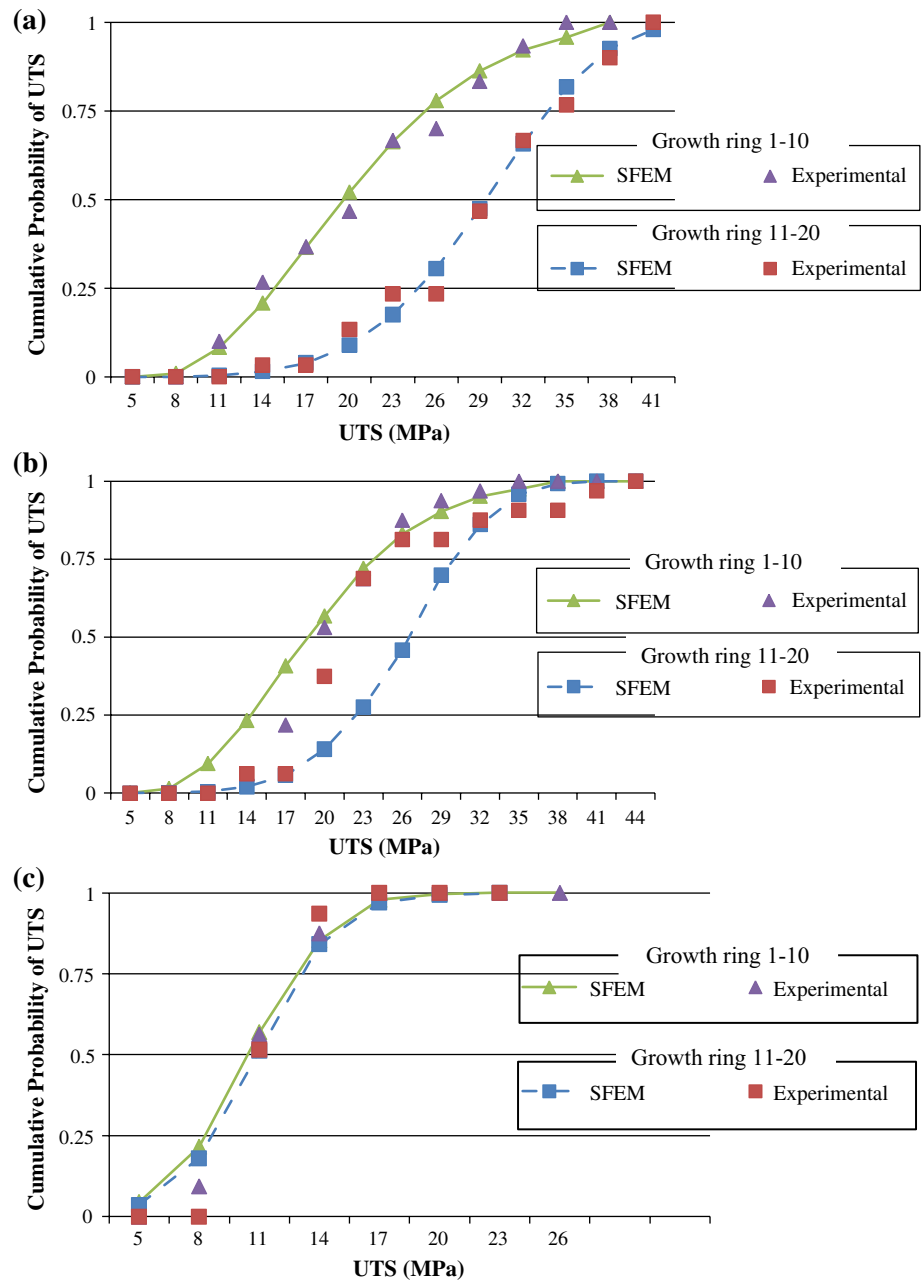
in the table indicate a correlation above 0.5 between the corresponding input variable and UTS. For growth ring number 1–10, UTS from radial grain strands was highly correlated with the longitudinal tension strength (Y_t). UTS from the tangential grain strands was highly correlated with earlywood MOE, latewood Poisson ratio, σ_y, and Y_t. UTS from angled grain strands was highly correlated with transverse tension strength (X_t). For growth ring number 11–20, UTS from radial grain strands was correlated with the latewood MOE, latewood Poisson ratio, σ_x, σ_y, τ_{xy}, and Y_t. UTS from tangential grain strands was correlated with the earlywood MOE, earlywood Poisson ratio, σ_x, σ_y, τ_{xy},

and Y_t. UTS from angled strands was correlated with latewood MOE, latewood Poisson ratio, σ_x, σ_y, τ_{xy}, and X_t.

The UTS values associated with the different strand orientations and growth ring numbers showed different responses to the input variables. Strands from growth ring number 1–10 had a higher correlation between the strength indexes and UTS values. Strands from growth ring number 11–20 had a higher correlation between the stress components and UTS. Material properties of earlywood and latewood from growth ring number 11–20 had higher values than from growth ring number 1–10, which caused greater stress y distributions (Fig. 2). Longitudinal strength

Table 3 Sensitivity analysis of input variables on UTS of different orientation strands

Sample	Earlywood		Latewood		Stress components			Strength indexes		
	E_L	v_{LR}	E_L	v_{LR}	σ_x	σ_y	τ_{xy}	X_t	Y_t	S
Growth ring number 1–10										
Radial	−0.28	−0.24	−0.41	−0.37	−0.45	−0.49	0.43	−0.01	*0.84*	0.01
Tangential	−0.48	−0.41	−0.18	−0.18	−0.09	*−0.52*	0.01	0.11	*0.79*	−0.02
Angled	−0.27	−0.26	−0.19	−0.16	−0.09	−0.31	−0.28	*0.76*	0.41	0.07
Growth ring number 11–20										
Radial	−0.27	−0.23	−0.69	−0.63	−0.58	−0.74	*0.57*	−0.02	*0.62*	0.03
Tangential	*−0.74*	*−0.71*	−0.24	−0.23	−0.66	−0.79	−0.74	0.19	*0.51*	0.07
Angled	−0.28	−0.27	*−0.57*	*−0.64*	*−0.72*	*−0.68*	*−0.55*	*0.60*	0.11	0.06

Italicized values indicate Spearman correlation coefficient (r) above 0.5

index (Y_t) of growth ring number 11–20 was 41% greater than growth ring number 1–10, which was much greater than the growth ring number 11–20 values of X_t and S, which were 16.2 and 13.9% less, respectively (Table 1). This change in the Y_t value caused the increase of sensitivity of stress components by minimizing the solution and predicted UTS from Eq. 3.

Latewood MOE and Poisson ratio were highly correlated with UTS of radial and angled orientation strand models from growth ring number 11–20. Earlywood MOE and Poisson ratio, however, had higher correlation with the UTS of tangential orientation strand model from growth ring number 11–20. Compared to the other orientation models, the physical geometry of tangential orientation strand models showed that one individual latewood or earlywood band failure was more susceptible in similar stress level to cause strand failure. The smallest longitudinal stress difference between earlywood band and latewood band was shown in the tangential orientation models that evidenced the high sensitivity of earlywood material properties on the UTS (Fig. 2). Longitudinal strength index (Y_t) had a strong correlation with the UTS of radial and tangential orientation model because the loading direction and fiber orientation were coincident. The transverse strength index (X_t) had a strong correlation with the UTS of angled orientation models because the loading direction and fiber orientation were not coincident.

Conclusions

UTS of different orientation wood strands was predicted from homogeneous model, deterministic layer FEM models, and probabilistic SFEM models. Comparison of average UTS from experimental results and models indicated that homogeneous models were not as accurate as layered FEM and SFEM models. Stress distributions associated with the homogenous models were not representative for physical wood structures that composed of earlywood and latewood bands. Radial, tangential, and angled grain orientation models showed less longitudinal stress distributions in earlywood bands and greater longitudinal stress distributions in latewood bands except for homogeneous models. Comparison between cumulative probability of UTS from experimental test and that of predicted UTS from SFEM showed no significant difference. UTS of radial, tangential, and angled grain orientation strands from the two different growth ring numbers showed a quite different sensitivity on input variables showing that UTS of strands from growth ring number 1–10 had a high sensitivity on strength indexes, whereas UTS of strands from growth ring number 11–20 had a high sensitivity on stress components and strength indexes. Different grain orientation also affected the sensitivity of UTS of different orientation strands. Longitudinal strength index (Y_t) had a strong correlation with UTS of radial and tangential grain orientation strands, whereas transverse strength index (X_t) had a strong correlation with UTS of angled grain orientation strand.

References

1. Larson PR, Kretschmann DE, Clark A III, Isebrands JG (2001) In: Gen Tech Rep FPL-GTR-129. USDA Forest Products Laboratory, Madison, WI
2. Bendtsen BA (1978) Forest Prod J 28(10):61
3. Cave ID, Walker JCF (1994) Forest Prod J 44(5):43
4. Panshin AJ, Zeeuw CD (1980) Textbook of wood technology. McGraw Hill, New York
5. Smith RW, Briggs DG (1986) In: Proceedings of cooperative technical workshop. Forest Products Research Society, Madison, WI, pp 1–11
6. Jeong GY, Zink-Sharp A, Hindman DP (2009) Wood Fiber Sci J 41(1):51
7. Jeong GJ (2008) Tensile properties of loblolly pine strands using digital image correlation and stochastic finite element method. Jeong, Blacksburg, VA

8. Kasal B, Leichti RJ (2005) Prog Struct Eng Mater 7(1):3
9. Chakraborty S, Dey SS (2000) Shock Vibration 7(5):309
10. Chung DB, Gutiérrez MA, Borst RD (2005) Comput Methods Appl Mech Eng 194(12–16):1427
11. Clouston P, Lam F (2002) Compos Sci Technol 62:1381
12. Eiermann M, Ernst OG, Ullmann E (2005) In: Proceedings of conference on scientific computing (Algoritmy 2005), 13–18 March 2005, Vysoke Tatry, Podbanske, pp 1–10
13. Ghanem RG, Spans PD (1991) Stochastic finite elements: a spectral approach. Springer-Verlag, Berlin
14. Ghanem RG (1999) ASME J Heat Transfer 121:290
15. Kaminski M (2002) Eng Comput 19(7):854
16. Kleiber M, Hien T (1992) The stochastic finite element method basic perturbation technique and computer implementation. Wiley, New York
17. Wang YT, Lam F (1998) J Comput Mater Sci 11:157
18. Clouston P (2007) Holzforschung 61:394